Magnetism of ultrathin wires suspended in free space and adsorbed on vicinal surfaces

D. Spišák* and J. Hafner
Institut für Materialphysik and Center for Computational Materials Science, Universität Wien, Sensengasse 8/12, A-1090 Wien, Austria
(Received 4 November 2002; revised manuscript received 10 April 2003; published 12 June 2003)

On the basis of total-energy calculations within density functional theory the possibility of magnetic ordering in ultrathin, one or two atom wide nanowires is studied. Specifically, we investigate nanowires composed of fifth and sixth row elements, which are nonmagnetic in the solid phase. At first, the unsupported straight wires are discussed and then, similar to experimental conditions, the wires are placed along step ledges of vicinal surfaces of copper and silver. Free-standing wires show only a weak tendency towards magnetic ordering at the equilibrium bond length. In analogy with their 3*d* homologues Mo, Tc, W, Re are found to order antiferromagnetically, Ru, Rh, and Ir ferromagnetically. Surprisingly, ferromagnetism is also predicted for the early transition metals Zr and Ta and for the simple metals In and Tl. This picture is profoundly modified for supported wires, where the expansion of the bond length enforced through the epitaxial relationship with the substrate favors magnetic ordering but hybridization with the substrate electrons tends to quench magnetism. It turns out that wires on a Cu substrate prefer a ferromagnetic order, whereas on a Ag substrate most elements tend to antiferromagnetism. A second row of atoms added to the wires destroys the magnetism in wires on a Cu substrate, and reduces it in wires on a Ag substrate, except for the late transition metals (Rh, Ir) where an enhancement of magnetic moments is observed. Two possible growth modes of nanowires — a row-by-row growth and island growth — are explored. The results allow us to suggest that Ru, Rh, and Os wires on Ag stepped surfaces are the most promising systems in which magnetism could be verified experimentally.

DOI: 10.1103/PhysRevB.67.214416 PACS number(s): 73.22.−f, 75.75.+a, 81.07.Vb, 81.16.Dn

I. INTRODUCTION

The study of magnetism at the nanometer scale has been an exceptionally active research area over the past years. Originally, plenty of work has been carried out on naturally formed quasi-one-dimensional magnetic chains in three-dimensional compounds.[1] Recently, the progress achieved in the fabrication of artificial nanostructures enabled the preparation of extended ultrathin nanowires which are uniform in thickness and perfect at the atomic scale. The fundamental idea is to exploit the geometrical restriction imposed by an array of parallel steps on a vicinal surface along which the deposited material can nucleate, a process called the step decoration. This method has been used to produce stripes of Fe on stepped W(110),[2] Cu on stepped Mo(110) and W(110),[3] Fe on stepped Cu(111),[4] Co on stepped Au(111),[5] or Ag, Cu (Ref. 6) and Co (Refs. 7,8) on Pt(997). The wire width and the interwire spacing can be controlled easily via dosage and miscut angle, respectively. The magnetic properties of the wires were found to depend strongly on the perfection of the wires. For Fe wires on stepped Fe(111) surfaces, Shen *et al.*[4] reported formation of rather irregular, fragmented stripes which showed a time-dependent magnetization, i.e., essentially a superparamagnetic behavior. On the other hand, Fe wires on W(110) show a sharp magnetic ordering transition.[2] Ferromagnetic behavior was also reported for nearly perfectly monoatomic wires of Co, formed at the steps of Pt(997) surfaces.[8]

Short suspended nanowires have been produced by driving the tip of a scanning tunneling microscope into contact with a metallic surface and subsequent retraction, leading to the extrusion of a limited number of atoms from either tip or substrate.[9,10] An alternative method uses a mechanically controllable break junction.[11] For these monoatomic wires (the technique works best for highly ductile metals such as gold), quantized electrical conductance has been reported.

Theoretical studies of magnetism in one-dimensional structures are still rather scarce and the existence of magnetic order in one-dimensional systems is still somewhat controversial. For a linear chain of three-dimensional atoms where only one orbital per atom contributes to the conductivity, a nonmagnetic ground state was predicted.[12] This result was confirmed by the Lieb-Mattis theorem[13] which excludes a magnetically ordered ground state for a one-dimensional one-band system. However, this theorem does not apply if two or more transverse subbands are occupied. To our knowledge, the first self-consistent band-structure calculation for an one-dimensional metallic system has been performed by Weinert and Freeman[14] studying iron and nickel wires. Assuming a bond length equal to the nearest-neighbor distance in the bulk, strong ferromagnetism with enhanced moments was concluded. It is well established that the origin of magnetic ordering is a direct or indirect exchange interaction between electrons in the partially filled *d* or *f* electronic shells. Interesting enough, for electrons confined in both lateral dimensions, as in a wire geometry, magnetism has been predicted for *sp*-bonded simple metals[15] within the stabilized jellium model. These conclusions have been backed by first-principle calculations of aluminum wires which indeed assume a small magnetic moment,[16] and by the theoretical investigation of gallium wires on Si(001) reporting a magnetic minimum-energy state in one of the considered wire geometries.[17] Bergara *et al.*[18] have investigated the structural, electronic and magnetic properties of sodium wires. A metallic, zig-zag ground state was predicted as the result of Jahn-Teller distortion and for chains under tensile stress a ferromagnetic ground state was found. It was shown that ferromagnetism results from the occupation of a second subband as the wire is stretched — hence the validity of the Lieb-Mattis theorem is not challenged by this result. Nearer to our interest here, Bellini *et al.*[19] have studied the magnetic

properties of monoatomic wires formed by 4*d* transition-metal atoms on several stepped Ag substrates. Eisenbach *et al.*[20] have examined the magnetic properties of Fe wires embedded in a Cu matrix, and the present authors have investigated the magnetic properties of Fe wires on stepped Cu substrates.[21] It was shown that the combined effect of the magnetic coupling between neighboring wires through the conduction electrons of the substrate and of the magnetic anisotropy leads to a magnetic ordering transition at ambient temperatures. The critical exponent characterizing the transition is found to be close to the value expected for the anisotropic *XY* model—confirming the effective two-dimensional character of an regular array of magnetic wires on a nonmagnetic metallic substrate.

The present work is devoted to the search for magnetic states in wires (both as free-standing wires and supported on metallic substrates) composed of elements from the fifth and sixth row of the Periodic Table, including the transition metals and the post-transition elements. None of these species is magnetic in the bulk. Nonetheless, it was pointed out that for some of these elements a spontaneous magnetization should appear if their dimensionality is reduced, e.g., large magnetic moments were calculated for monoatomic Ru, Rh, and Ir overlayers on Ag(001)(Ref. 22) and for Mo and Tc wires on Ag(117) vicinal surfaces.[19] Both free-standing wires and wires deposited along the steps on the surface of the substrate are considered. At this point it should be made clear that weak coupling between neighboring wires via the conduction electrons of the substrate adds a new dimension to the problem: even if a free-standing one-dimensional chain does not order magnetically at nonzero temperature, there is still the possibility that the interwire coupling induces a magnetic ground state. We have estimated previously the interwire magnetic coupling in Fe wires on a stepped copper template to be of the order of a few meV.[21] Such a coupling combined with a sizable intrawire coupling and the magnetic anisotropy seems to be sufficient to stabilize a Curie temperature as high as 200–300 K.

In the following section we give a concise outline of the methods used in our study and a description of the computational setup. In Sec. III we present a systematic study of the binding energies and the collinear magnetic structures found in unsupported linear wires. Section IV summarizes the results obtained for wires grown along steps on Cu(117) and Ag(117) surfaces and Sec. V is devoted to the discussion of structural stability of monoatomic wires and to the relationship between the wire thickness and its magnetic behavior. The conclusions are given in Sec. VI.

II. COMPUTATIONAL DETAILS

The calculations have been performed within the framework of spin-polarized density functional theory. We used the Vienna *ab initio* Simulation Package VASP(Ref. 23) in a projector augmented-wave (PAW) representation, which is as accurate as frozen-core all-electron methods.[24,25] Exchange and correlation effects were described by the local functional due to Perdew and Zunger,[26] employing the spin-interpolation proposed by Vosko *et al.*[27] and adding generalized gradient corrections.[28] The cutoff energy of the plane wave basis set varied depending on the chemical element, we applied the default values tabulated for the PAW potentials.[29] The mass-velocity and Darwin correction terms are incorporated into potentials, but spin-orbit relativistic effects are neglected in this study. It has been documented in some previous theoretical studies that the inclusion of a spin-orbit coupling can slightly modify bond lengths,[30] and eventually even change the character of a wire from metallic to insulating.[31] However, this last result corresponded to the special case of Pb wires, where the Fermi level happens to fall into the gap between the $p_{1/2}$ and $p_{3/2}$ bands created by the spin-orbit splitting. Regarding magnetic properties, the spin-orbit interaction determines a magnetocrystalline anisotropy energy, but does not influence a size of magnetic moments, presented here, in a significant way.

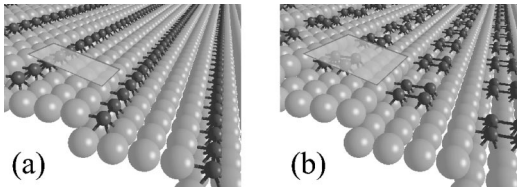

FIG. 1. Pictorial view of stepped (117) surface. In the left picture monoatomic row of atoms along the steps is depicted, the right picture represents the surface with small clusters. The surface cells of the models used in calculations are shown as semitransparent quadrilaterals.

A free-standing wire was modeled by a chain of atoms in a periodically repeated box with lateral dimensions of 20 Å , that turned out to be wide enough to decouple neighboring wires. The slab thickness equal to the doubled atomic bond length (in order to allow for an antiferromagnetic configuration) was considered as a variable parameter. The integrations over the one-dimensional Brillouin zone were carried out with 12 special *k* points.[32]

The (117) vicinal surface of a face centered cubic crystal consists of regular array of straight steps along the $[\bar{1}10]$ direction with four-atom wide terraces of (001) planes between them. The face of a decorated (117) substrate and the basic surface cell used in our calculation are depicted in Fig. 1(a). The model was built up as a stack of eight (001) planes tilted by 11.42° away from the [001] direction and contains 56 substrate atoms plus four wire atoms, two of them on each side of the slab. The total energy convergence with respect to the number of *k* points as well as with the thickness of the vacuum region separating the repeated slabs was tested for ferromagnetic Ru wires on Ag(117). We have compared total energies obtained for 6, 9, and 14 *k* points for a vacuum measuring 5 (001) interlayer distances. While a total energy difference of 44 meV/Ru atom between the calculations with 6 and 14 *k* points was found, the results for 9 and 14 *k* points differ only by 4 meV/Ru atom. Convergence with respect to the thickness of the vacuum region is faster, the difference in the total energies obtained for the thinnest and the thickest vacuum region (5 and 11 interlayer distances, respectively) amounts merely to 3 meV/Ru atom. Our hands-on experience with this type of calculations allows us

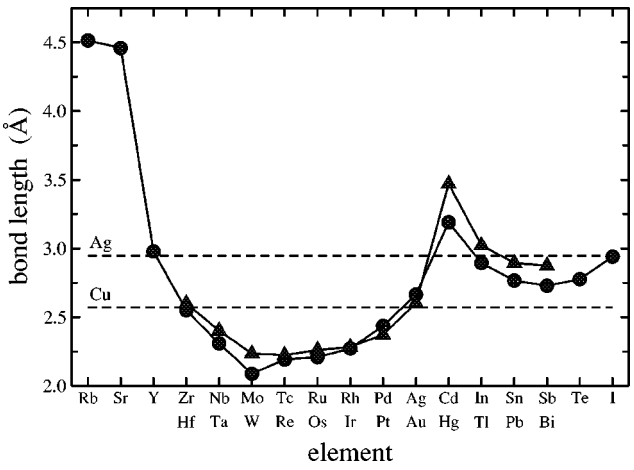

FIG. 2. Equilibrium bond lengths of the straight nonmagnetic wires composed of the fifth-row (circles, Rb to I) and sixth-row (triangles, Hf to Bi) elements. The dashed lines denote the interatomic distances in bulk copper and silver.

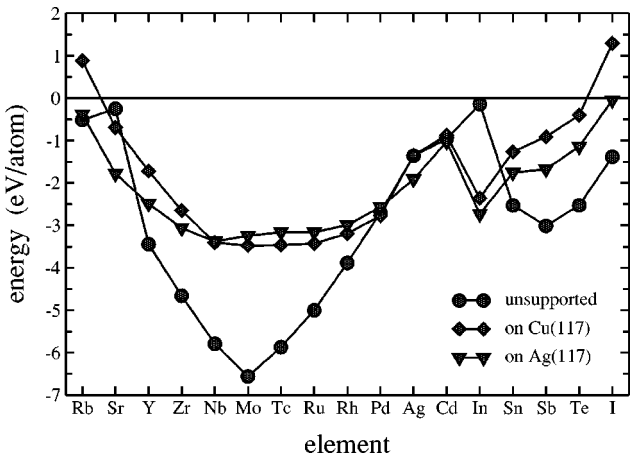

FIG. 3. The binding energies of unsupported wires (circles) taken with respect to isolated spherical atoms as reference, and the chemical binding energy between wire and substrate according to Eq. (1) (triangles and squares) for the fifth-row monoatomic wires on stepped Cu(117) and Ag(117) substrates.

to claim that with the setup we have used in the rest of the present study, namely 9 k points and vacuum space equivalent to five atomic layers, a numerical convergence of 2 meV/wire atom in the *relative* energies between different magnetic phases can be achieved. The variation in magnetic moments was below 5%. In some calculations models with two times larger surface cell were adopted. In these cases the slab thickness was reduced to six (001) planes leading to 92 atoms in the cell, inclusive wire atoms, and 2 k points in the irreducible Brillouin zone were used.

III. FREE-STANDING CHAINS

A. Bonding and electronic structure of straight nonmagnetic chains

We turn first to the unsupported wires — this will allow us to distinguish between effects coming from the intrawire interactions alone and those ensuing from the wire-substrate interaction. The results of non-spin-polarized calculations for the equilibrium bond distance against the band filling are shown in Fig. 2, the variation of the binding energy is shown in Figs. 3 and 4. The shortest bonds are formed between Mo atoms amongst the fifth row elements and Re atoms in the sixth row. Common to both are precisely half-filled d bands. The trends of the bond weakening and the cohesive energy reduction in going from the middle of both series to atoms with highly open or nearly closed d shells was explained by Friedel assuming a constant density of states of d electrons.[33] The binding energy shown in Figs. 3 and 4 behaves in a similar fashion — the filling of the bonding $4d$ and $5d$ states of early transition metals increases the binding energy and an additional filling of the antibonding states reduces it again. Deviations from the ideal parabolic behavior reflect the one-dimensional nature of the structure, as the binding energies of transition-metal dimers reveal a marked triangular variation against the band filling.[33] Bonding is much weaker in wires formed by sp elements, the most loosely bonded are s-valent Rb and Sr wires. Elements with partially filled p bands follow a trend similar to that observed for the transition elements, the bonding is strongest for Sb and Bi with a half-filled p band.

The variation of the electronic structure across the $4d$ series is shown in Fig. 5. Essentially the density of states (DOS) consists of a superposition of subbands of marked one-dimensional character with a pronounced van Hove singularity at the lower edge of each band. Close to the band edge E_b the DOS varies roughly as $1/\sqrt{E-E_b}$. The lowest band has essentially $ss\sigma$ and $dd\sigma$ character, it is composed of s and d_{z^2} orbitals extending along the chain (which defines the z direction). For the early transition metals, the $ss\sigma$ and $dd\sigma$ bands are quite distinctly separated. With increasing band filling, the d_{z^2} states are lowered in energy with respect to the s states and the two bands merge into a single s-d_{z^2} hybridized band. The $dd\pi$ coupling between d_{xz} and d_{yz} states leads to the formation of a very broad band whose bonding part dominates at larger binding energies. The $d_{x^2-y^2}$ and d_{xy} orbitals extending in the plane perpendicular to the chain are only relatively weakly coupled through $dd\delta$

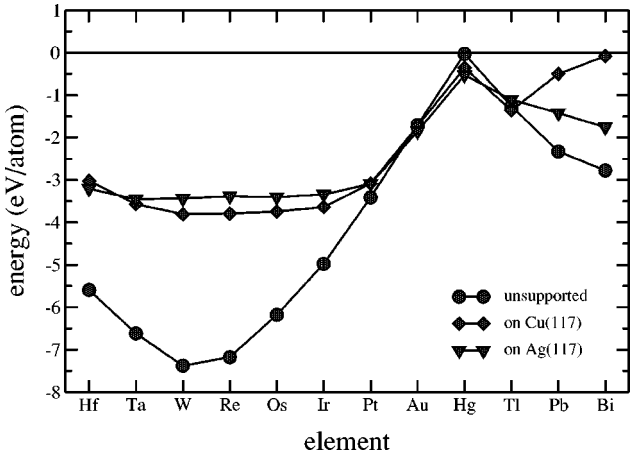

FIG. 4. The same as in Fig. 3, but across the sixth-row elements.

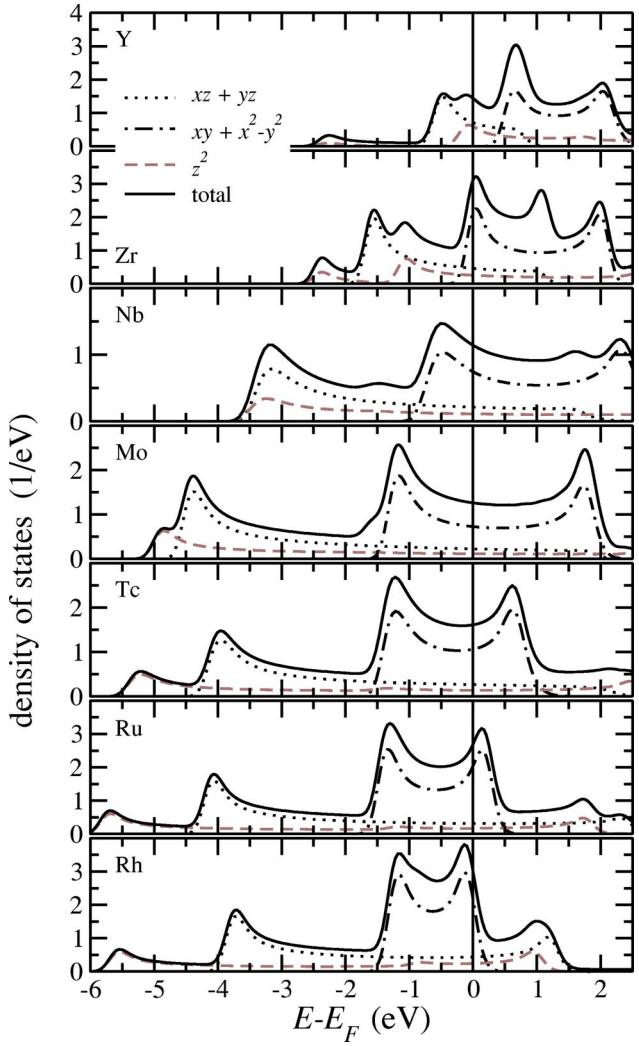

FIG. 5. Paramagnetic density of states of the 4*d* elements from Y to Rh calculated for wires with the respective equilibrium bond length. Full lines: total DOS, dotted lines: the $d_{xz,yz}d_{xz,yz}\pi$ partial DOS, dot-dashed lines: $d_{xy,x^2-y^2}d_{xy,x^2-y^2}\delta$ partial DOS, dashed lines: the $d_{z^2}d_{z^2}\sigma$ partial DOS. The *z* direction is parallel to the wire axis.

interactions, leading to the formation of a narrower band centered around the Fermi level. With increasing filling of the *d* band, the Fermi energy shifts from the lower to the upper edge of the $dd\delta$ band. In Zr we find a maximum of the paramagnetic DOS at the Fermi level — if we admit the validity of a Stoner picture for magnetic ordering, this suggests that a Zr chain could be ferromagnetic. In Mo and Tc the Fermi level falls right into the DOS minimum separating bonding and antibonding states — in analogy to bulk Cr and Mn, these metals could order antiferromagnetically. In Ru and Rh we find again a high DOS at E_F, suggesting the possibility of ferromagnetic ordering. Hence the symmetric shape of the subband DOS in the one-dimensional chains which contrasts the asymmetric DOS of the hexagonal close packed and face centered cubic early and late transition metals could lead to a variation of the magnetic ground state from ferromagnetism (FM) to antiferromagnetism (AFM) and back to ferromagnetism with increasing band filling.

TABLE I. The calculated bond distances d_0, the magnetic moments *m*, and the energy differences ΔE_{mag} with respect to the nonmagnetic ground state for linear wires. The occurrence of metastable magnetic configurations at expanded distances is marked by the larger than sign. Abbreviations: ferromagnetic state (FM), antiferromagnetic state (AFM), nonmagnetic state (NM).

element	FM			AFM			NM
	d_0 (Å)	m (μ_B)	ΔE_{mag} (meV)	d_0 (Å)	$\lvert m\rvert$ (μ_B)	ΔE_{mag} (meV)	d_0 (Å)
Y	>3.00						2.98
Zr	2.55	0.38	−25				2.55
Nb	>2.36			>2.31			2.31
Mo	>2.32			2.15	1.48	−92	2.09
Tc	>2.27			2.30	1.93	−65	2.19
Ru	2.23	0.98	−39	>2.32			2.21
Rh	2.27	0.26	−6	>2.57			2.27
In	2.94	0.30	0				2.89
Hf	>2.92						2.60
Ta	2.42	0.68	−20				2.40
W	>2.42			2.27	1.36	−3	2.24
Re	>2.33			2.30	1.89	−106	2.22
Os	>2.27			>2.31			2.26
Ir	2.29	0.64	−32	>2.65			2.28
Pt	>2.65			>2.76			2.37
Tl	3.06	0.26	−4				3.02

This differs from the behavior of the bulk 3*d* metals, where ferromagnetism exists for metals with a more than half-filled band and antiferromagnetic order is stabilized for metals with a less than half-filled band, but the early 3*d* metals are nonmagnetic.[34]

Bonding in the transition-metal wires may also be analyzed in terms of the crystal-orbital overlap populations (COOP's).[35] Basically, we find that the bonding is entirely dominated by *d*-*d* interactions, with negligible contributions from *s* and *p* states. For $dd\sigma$, and $dd\delta$ interactions the COOP's change sign at or very close to the Fermi energy, demonstrating that the chemical bond strength is maximized by populating only bonding states. On the other hand, the occupied $dd\pi$ states around the Fermi level are of antibonding character.

B. Magnetic ground state of transition-metal wires

Spin-polarized calculations confirm the trend suggested by the analysis of the paramagnetic DOS. The magnetic moments and the bond lengths of either the ground-state solutions or the bond length corresponding to the onset of magnetism are listed in Table I. If no entry is listed in the table, the corresponding magnetic state is unstable at any considered bond length. In the 4*d* series Zr, Ru, and Rh wires are predicted to order ferromagnetically, Mo and Tc have an antiferromagnetic ground state. Nb is a border-line case, it orders antiferromagnetically under a very modest tensile strain. In the 5*d* series we observe essentially the same trend, but slightly shifted towards higher band filling: Hf is nonmag-

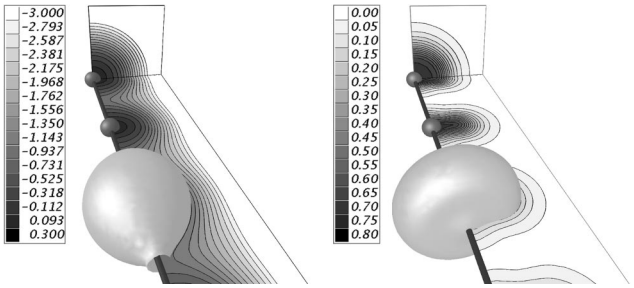

FIG. 6. 3D representation (isosurface and contour plots) of the charge (left panel) and spin (right panel) densities in a Mo wire. Note that charge overlaps to form a bond charge, but that the spin density is strongly confined along the direction of the wire. Charge distribution is plotted in a logarithmic scale. Isosurfaces correspond to the charge density of 0.4 $e/\text{Å}^3$ and spin density of $0.2\mu_B/\text{Å}^3$.

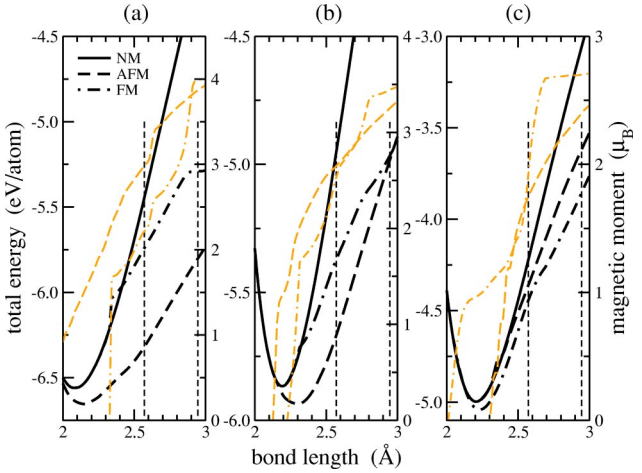

FIG. 7. Total energy (left-hand scale) and magnetic moment (right-hand scale) of (a) Mo, (b) Tc, and (c) Ru in all three magnetic configurations as a function of the bond length. The vertical lines mark the bond length on Cu ($d_{\text{Cu}}=2.57$Å) and Ag ($d_{\text{Ag}}=2.95$Å) substrates for comparison.

netic, Ta shows FM order, W and Re an AFM order, Ir again a FM ground state, Os orders ferromagnetically on very slight extension. The slight difference between the $4d$ and $5d$ metals is due to the more extended $5d$ orbitals leading to a larger bandwidth. The magnetic moments of the FM wires are quite modest, the largest moment is found for Ru with about $1\mu_B$, the magnetic energy difference is generally smaller than 40 meV/atom. The moments are substantially larger in the wires with an AFM ground state. For all metals we find a modest magnetoelastic effect — magnetic ordering induces an increase of the equilibrium bond length in the range from 0.01 to 0.11 Å .

As suggested by the paramagnetic DOS (see Fig. 5), the spin density shown at the example of a Mo wire in Fig. 6 is almost entirely of d_{xy} and $d_{x^2-y^2}$ character: an isosurface has essentially the form of an oblate, rotationally symmetric ellipsoid extending perpendicular to the direction of the wire. This result is important in two respects: it shows that the result that magnetic ordering in one-dimensional systems depends on the partial occupation of one or more transverse subbands remains valid for *d*-bonded chains, and it suggests that the magnetism of wires will be strongly influenced by interactions with the substrate.

All the elements listed in Table I order ferromagnetically under a sufficiently large tensile strain, the AFM order is also stabilized on extension, but not for metals with a nearly empty *d* band (Y, Zr, Hf, Ta). For metals with a nearly full *d* band a stable or metastable FM state coexists with metastable AFM configuration at a higher energy. Figure 7 displays the variation of the total energy and of the magnetic moment of all three magnetic configurations at the example of Mo, Tc (both have an AFM ground state), and Ru (a FM ground state). In Mo a metastable ferromagnetic state coexists with the antiferromagnetic configuration for bond lengths larger than about 2.5 Å . The energy difference between the two magnetic configurations begins to decrease if the interatomic distance becomes larger than ~2.9 Å . A similar trend is seen for Tc — here the magnetic energy difference between the FM and AFM configurations vanishes at an interatomic distance comparable to that on an Ag substrate. This indicates the possibility that the magnetic ground state of a supported Tc wire depends on the lattice parameter of the substrate. For Ru wires we find a metastable antiferromagnetic state for extended wires. The magnetic energy difference remains small up to a bond length of about 2.6 Å , further extension stabilizes the ferromagnetic configuration. The trend towards ferromagnetism in stretched wires is related to the progressive band narrowing leading to an increase of the paramagnetic DOS at E_F so that a generalized Stoner criterion is satisfied.

The variation of the magnetic moment with the bond length reveals that the increase is rather steep, almost discontinuous at certain interatomic distances — this happens when one of the van Hove singularities of the narrowed subbands passes through the Fermi level. In an extended Mo wire with a bond length of ~3 Å , the magnetic moment reaches a value of $4\mu_B$ corresponding to the maximum of the magnetic moment according to Hund's rule, assuming a fully occupied *s* band. In reality, however, the *s* character of the conduction band is quite small and the moment continues to increase upon further extension. The stepwise increase of the magnetic moment, which occurs at different bond lengths for the FM and AFM phases, is also the reason for the nonmonotonous variation of the magnetic energy difference with the bond length.

C. Magnetic ground state of *sp*-bonded wires

All noble metals and *B*-group metals with closed *d* shells remain nonmagnetic even under tensile strain, with the exception of In and Tl. In these two elements which have one unpaired $5p$ or $6p$ electron, respectively, the ferromagnetic and nonmagnetic phases can coexist. The reason for the magnetic order is obvious from the density of states plotted in Fig. 8. As the *s* and *d* subbands in the transition metals, the $ss\sigma$, $pp\sigma$ (p_z), and $pp\pi$ (p_x,p_y) subbands show characteristic van Hove singularities at the bottom of each subband followed by a $1/\sqrt{E-E_b}$ decay. Since in the paramagnetic state the van Hove singularity of the $pp\pi$ subband falls al-

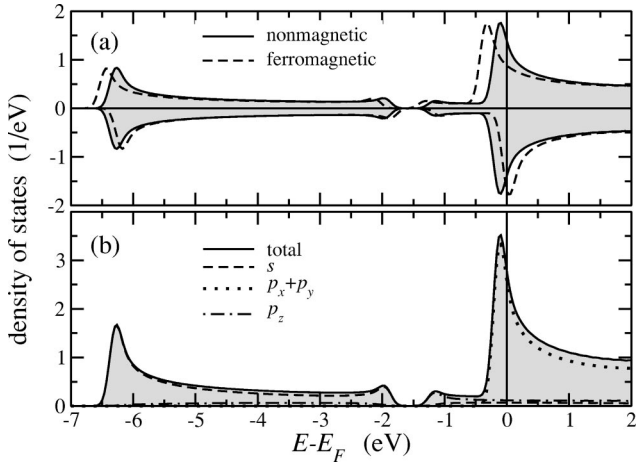

FIG. 8. (a) Paramagnetic (solid lines and filled area) and ferromagnetic (dashed lines) density of states of a sp-bonded straight monoatomic indium wire. (b) Partial s, $p_{x,y}$, and p_z DOS of a paramagnetic In wire.

most on the Fermi energy, spin-polarization splitting of the DOS peak is energetically favored.

Ayuela *et al.*[16] have performed selfconsistent calculations for free-standing Al wires. For a straight chain, the ground state was found to be nonmagnetic, but a ferromagnetic state develops in a wire stretched by about 10% compared to the equilibrium bond length. The magnetic moment in the expanded wires is about twice as large as for the ferromagnetic ground state of the In wires.

Similar van Hove singularities exist also in the jellium model of the free-electron gas confined within a cylinder, serving as a model of a monoatomic wire[15] and in the DOS reported by Bergara *et al.*[18] for a zig-zag chain of Na atoms. There are, however, important differences between these three cases: for In and Tl with three valence electrons, the existence of a van Hove singularity close to the Fermi level is the natural consequence of the incipient occupation of the p band. For the alkali metal Na, the partial occupancy of the lowest p band is the result of the zig-zag geometry of the chain inducing a strong sp hybridization. As the zig-zag wire is stretched and the bond angle increased, the hybridization is reduced, the p band is emptied and the wire becomes nonmagnetic.[18] For the jellium model, the number of van Hove singularities (corresponding to the number of subbands) in the occupied part of the band depends strongly on the assumed radius of the cylinder to which the electron gas is confined. As the radius is increased at a constant electron density, ferromagnetic and paramagnetic solutions alternate. In particular, a fully spin-polarized ground state is predicted when only the lowest subband is occupied. Altogether, the physics leading to the formation of a magnetic ground state is quite different in the jellium model and in calculations accounting for the true atomic structure.

D. Polymerization and distortions

It has been pointed out repeatedly that straight one-dimensional chains are unstable against polymerization and/or zig-zag formation: Bergara *et al.*[18] have demonstrated that a zig-zag configuration is the structural ground state of Na wires (and important to induce a partial population of the transverse p band leading to the formation of a FM ground state). Ayuela *et al.*[16] have shown that zig-zag formation at a fixed bond length also lowers the total energy of Al wires (but reduces the magnetization considerably), the zig-zag configuration is also stable if the wire is deposited on a substrate such as NaCl(001) on which it is only weakly bound. Similar surface polymerization reactions have also been reported by Brocks *et al.*[36] for Al and by Okada and Oshiyama[17] for Ga adsorbed on Si(001). For free-standing Fe wires the present authors have shown[21] that dimerization leads to a marginal gain in energy, whereas bending into a zig-zag form at a constant interatomic distance lowers the energy of a ferromagnetic wire by as much as 1 eV/atom, at an almost unchanged magnetic moment. At equilibrium, a stripe of almost equilateral triangles is formed. The focus of the present work is on wires formed at the steps of (117) surfaces of face centered cubic metals. The terraces on these surfaces have a square geometry, hence a zig-zag wires will not represent a favorable geometry for wire-substrate interaction. For this reason we have not investigated possible distortions of the free-standing wires, but confined our attention to possible structural instabilities of the adsorbed wires.

IV. MONOATOMIC WIRES ON CU(117) AND AG(117)

A. Stability

We can now proceed to the results for wires decorating vicinal (117) surfaces of face centered cubic metals, as depicted in Fig. 1(a). The steps run along the [110] direction, in the "step notation" introduced by van Hove and Somorjai[37] this is a $(001)\times(111)$ step [i.e., the terraces form (001) facets, the step edges (111) microfacets]. The step is close packed so that the atoms along the step edge are nearest neighbors, their coordination number is 7. As substrates of interest we have picked out the monovalent noble metals copper and silver due to their low reactivity, and on which uniform step arrays can be prepared. In addition, their interatomic distances ($d_{\mathrm{Cu}}=2.572$ Å and $d_{\mathrm{Ag}}=2.946$ Å , the calculated values) fit the equilibrium bond length along the step edges of Cu(117) and Ag(117) quite well (cf. Fig. 2). Only for the metals from the middle of the transition-metal series a tensile strain has to be imposed to match the geometry of the substrate. Wires formed by the post-transition elements have to be compressed to fit the step edges on the Cu substrate, on Ag the mismatch is very small anyway. Throughout the calculations the wires were fixed in their ideal positions along the step edges and any relaxation of atomic positions was neglected.

As a measure of the stability of a wire on a stepped surface we define the energy difference

$$\Delta E=\frac{1}{2}[E(\mathrm{substrate+wire})-E(\mathrm{substrate})-E(\mathrm{wire})], \tag{1}$$

where the first two terms are the total energies of the decorated and clean substrate, the last term is the energy of the

TABLE II. The calculated magnetic moments m, the energy differences ΔE_{mag} with respect to the nonmagnetic ground state, and the Stoner parameters I for linear wires on Cu(117). The magnetic moments in parentheses were obtained for an unsupported wire with the interatomic bond length of d_{Cu}.

element	FM			AFM		
	m (μ_B)	ΔE_{mag} (meV)	I (eV/μ_B)	$\lvert m\rvert$ (μ_B)	ΔE_{mag} (meV)	I (eV/μ_B)
Mo	0.74 (2.22)	−46	0.75	0.99 (2.98)	−16	0.65
Tc	1.30 (2.54)	−48	0.72	1.27 (2.65)	−44	0.70
Ru	0.35 (1.95)	−5	0.67	0.12 (1.74)	0	0.73
W	0.54 (1.76)	−28	0.75	0.10 (2.73)	0	0.61
Re	0.50 (2.49)	−12	0.71	0.74 (2.66)	−3	0.63
Os	0.47 (1.94)	−11	0.64	− (1.66)		0.71

TABLE III. The calculated magnetic moments m, the energy differences ΔE_{mag} with respect to the nonmagnetic ground state, and the Stoner parameters I for linear wires on Ag(117). The magnetic moments in parentheses were obtained for an unsupported wire with the interatomic bond length of d_{Ag}.

element	FM			AFM		
	m (μ_B)	ΔE_{mag} (meV)	I (eV/μ_B)	$\lvert m\rvert$ (μ_B)	ΔE_{mag} (meV)	I (eV/μ_B)
Nb	0.79 (2.27)	−7	0.88	0.89 (1.86)	−20	0.82
Mo	2.36 (4.00)	−325	0.66	3.00 (3.86)	−512	0.66
Tc	2.68 (3.44)	−427	0.72	2.63 (3.25)	−451	0.72
Ru	2.11 (2.70)	−169	0.71	1.61 (2.40)	−76	0.71
Rh	0.71 (1.62)	−45	0.70	− (1.12)		
W	1.63 (3.37)	−147	0.66	2.30 (3.38)	−223	0.63
Re	1.88 (3.21)	−291	0.68	2.53 (3.39)	−351	0.66
Os	1.86 (2.92)	−29	0.68	1.41 (2.45)	−78	0.68
Ir	0.48 (2.14)	−9	0.64	− (1.46)		

wire calculated at the substrate lattice parameter. Thus, our definition of ΔE accounts for the chemical binding between wire and substrate, but not for the elastic energy E_{st} associated with a wire compression or expansion necessary to match the substrate geometry. As shown in Fig. 4, the chemical interaction with both substrates is attractive for the wires consisting of sixth-row elements. The addition of the strain energy E_{st} to the ΔE makes Hg and Bi wires unstable on Cu(117). For the $5d$ metals, the binding between wire and substrate is found to be almost independent of the band filling. If the elastic strain energy is added to ΔE, the energy of the wire is even least exothermic for a half-filled band.

Amongst the fifth-row elements Rb and I wires are predicted not to bind to Cu(117). Sr and Cd wires on Cu(117) and Rb on Ag(117) are destabilized when the elastic strain energy E_{st} is taken into account. For the $5d$ metals, the mismatch between the bond lengths of a free-standing wire may be as large as $\sim$0.5 Å on Cu and $\sim$0.9 Å on Ag for the metals with an about half-filled d band (see Fig 2). For a paramagnetic wire, the elastic strain energy on Ag(117) may be as large as 2 to 3 eV/atom and hence almost as large as the binding energy between wire and substrate. The increasing magnetic energy difference, however, strongly reduces the elastic energy and favors the formation of supported wires.

B. Magnetic ordering of supported monoatomic wires

The formation of additional bonds with the step atoms has a pernicious effect on the wire magnetization. On the other side, however, almost all wires, in particular those of transition metals are expanded upon a deposition onto the substrates, promoting this way a tendency towards magnetism. The results concerning the magnetic moments for both ferromagnetic and antiferromagnetic configurations together with the energy gains relative to the nonmagnetic solution are listed in Table II for wires on Cu(117) and in Table III for wires on Ag(117).

1. Wires on Cu(117)

Of the wires formed by adsorption along a step edge of Cu(117), only the metals with a half-filled d band are found to order magnetically: Mo, Tc, and Ru among the $4d$ metals and W, Re, and Os among the $5d$ elements. All these wires order ferromagnetically, although the magnetic ordering is stabilized only by a modest energy difference <50 meV/wire atom. These magnetic energy differences are comparable to those for unsupported wires at equilibrium, but more than one order of magnitude smaller than those obtained for free-standing wires with the same interatomic distance. The magnetic moments are also much smaller than calculated for unsupported wires of the same bond length, due to the increased coordination at a step edge.

The fact that metals with an approximately half-filled band order ferromagnetically is by itself rather surprising result — it is even more astonishing since in the form of free-standing wires Mo, Tc, W, and Re have an AFM ground state and Os is nonmagnetic. Solely Ru is FM in both forms. In the preceeding section we have shown that only for Tc the expansion of the chain leads to a reduction of the energy difference between the AFM and FM states — in all other cases, the change in the magnetic order must be induced by electronic interactions with the substrate.

Figure 9 shows the electronic density of states of Mo/Cu(117) and Mo/Ag(117) in the nonmagnetic, FM and AFM states as well as for a free-standing Mo wire with the bond length equal to that of Cu substrate. Compared to the equilibrium bond length, the DOS of the expanded isolated wire is strongly modified. In the nonmagnetic state, the total width of the occupied band is narrowed from 5 to 3 eV, all the structures associated with the subbands are much more pronounced (see Fig. 5). An expanded AFM Mo wire is even predicted to be insulating with a gap of about 0.6 eV. This is a combined consequence of the band narrowing and the formation of a large moment of nearly $3\mu_B$ and the correspondingly increased exchange splitting (see Fig. 7). An expanded FM Mo wire on the other hand is just beyond the nonmagnetic/ferromagnetic transition and remains metallic.

The DOS of a Mo wire on Cu(117) [but it applies also to Mo wire on Ag(117)] is strongly influenced by the d-d hybridization with the substrate. From spectroscopic investiga-

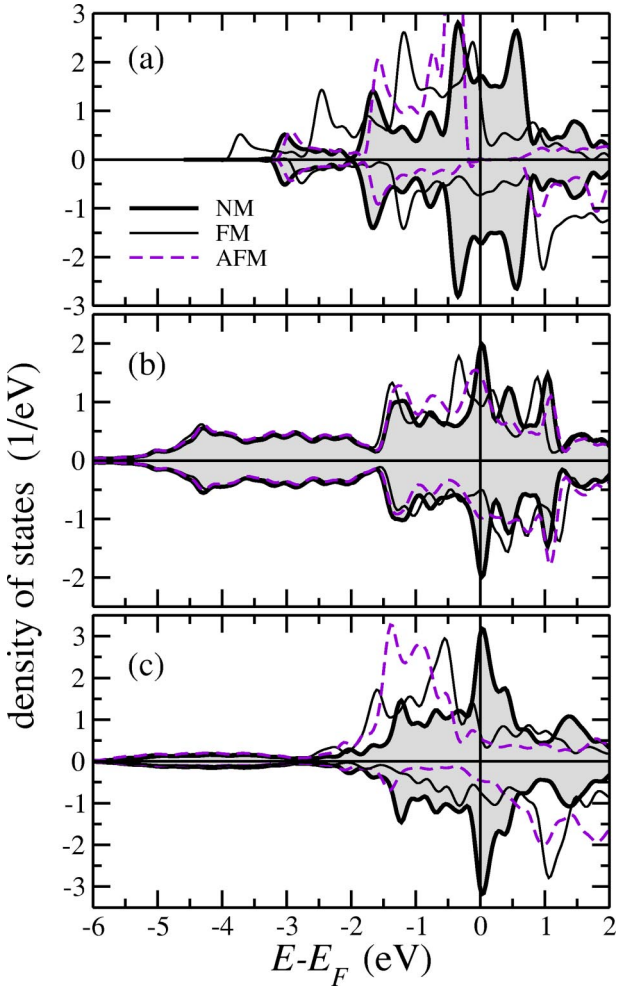

FIG. 9. Density of states of nonmagnetic (NM), ferromagnetic (FM), and antiferromagnetic (AFM) Mo in (a) free-standing wire with the interatomic distances corresponding to Mo/Cu(117) and in a wire supported on (b) Cu(117) and (c) Ag(117).

tions and electronic structure calculations on transition-metal alloys it is well known that the *d* band of the components repel each other: the *d* band of the metal with the larger band filling (in our case the noble metals Cu, Ag) is shifted to higher binding energies, the binding energy shift increases with the difference in the *d* band filling, both subbands are separated by a hybridization minimum in the DOS.[38,40] However, each component has a sizable minority contribution in the subband of the other metal. The transition-metal wires adsorbed on Cu conform with this general picture: we find a considerable Mo contribution located at binding energies between -5 and -1.5 eV. The *d* band of Mo is pushed to lower binding energies such that the DOS peak associated with the van Hove singularity at the lower edge of the $dd\delta$ band falls on the Fermi energy. This is a classical situation for a ferromagnetic instability according to the Stoner picture. Due to an exchange splitting of about 0.8 eV in Mo/Cu(117) electronic states, the Fermi energy falls into a DOS minimum in both the spin-up and the spin-down band, favoring FM ordering. In the AFM state, the spin-polarized DOS at the Fermi energy is large for both spin orientations. Therefore the hybridization with the Cu surface is able to turn the AFM ground state in an isolated wire to a FM ground state on Cu substrate. Upon further expansion experienced by a Mo wire on Ag(117) the most notable changes are a constriction of spin-up band in AFM state and a depletion of spin-down bands in both the AFM and FM states, which is more substantial in the AFM configuration, though. Due to these changes the AFM state is recovered.

Within the theory of itinerant magnets, the Stoner parameter I may be calculated in terms of the exchange splitting ΔE_{nd} (defined as the difference in the positions of the spin-down and spin-up components of the *d* bands, $n=4,5$) and the magnetic moment m as $I=\Delta E_{nd}/m$. For the magnetic wires on Cu(117) substrates we find only a small variation with band filling, I decreases slightly for FM wires and increases for AFM wires as the *d* band is filled. The average value of I is ≈ 0.7 eV/μ_B, to be compared with $I \approx 1$ eV/μ_B in bulk magnetic $3d$ metals and alloys.[39,40]

2. Wires on Ag(117)

For wires formed at the step edges of Ag(117) surfaces, we find a totally different picture as seen from Table III: all the wires that order ferromagnetically on Cu(117), except Ru, namely, Mo, Tc, W, Re, Os, and in addition Nb now have an antiferromagnetic ground state. The late transition metals Ru, Rh, and Ir order ferromagnetically. Hence we return to a scenario familiar from the $3d$ bulk metals — the FM order in free wires of early transition metals (Zr, Ta) does not appear in the wires on Ag(117). The energy gain due to magnetism is much larger than for wires supported on Cu; for Mo the magnetic energy difference is about the same as for the free wire with the same interatomic distance, for the other metals it is somewhat smaller.

Except for the border-line cases (Nb, Rh, Ir), wires on a Ag substrate display large magnetic moments ranging between 2 and $3\mu_B$ and correspondingly large exchange splitting. The Stoner parameter I has about the same value as for the wires on Cu showing much weaker magnetism. The almost constant value of the Stoner parameter suggests that an itinerant description of one-dimensional magnetism is adequate.

The magnetic properties of $4d$ monoatomic rows on Ag(117) substrates have been studied recently by the screened Korringa-Kohn-Rostocker Green's function method and the local spin-density approximation.[19] In spite of quite a different computational approach, their conclusions match our results reasonably well. Both methods find antiferromagnetism to be preferred for Nb and Mo wires, almost same stability of the ferromagnetic and antiferromagnetic states in Tc and ferromagnetism in Ru and Rh wires. Our study yields larger magnetic moments and larger magnetic energy differences. In addition we find metastable magnetic solutions for Nb and Ru, which have not been detected previously (the ferromagnetic solution for Nb wires, the antiferromagnetic solution for Ru wires). These differences are probably related to our use of gradient corrections to the exchange-correlation electronic potential, but not in the previous work, or to the atomic sphere approximation applied in that work.

TABLE IV. The calculated magnetic moments $m(m_1$: atoms in the first row immediately at the step edge, m_2: atoms in the second row), the magnetic energy differences ΔE_{mag} with respect to the appropriate ground state solution for biatomic wires on Cu(117). The rightmost column represents the energy difference $\Delta E = E(\mathrm{cluster}) - E(\mathrm{wire})$ of the structural models drawn in Fig. 1. The energies are given per wire atom. Abbreviations: ferromagnetic state (FM), checkerboard (2×2) antiferromagnetic state (C-AFM), row antiferromagnetic state (R-AFM), nonmagnetic state (NM).

element	FM ΔE_{mag} (meV) m_1, m_2 (μ_B)	C-AFM ΔE_{mag} (meV) $\lvert m_1\rvert$, $\lvert m_2\rvert$ (μ_B)	R-AFM ΔE_{mag} (meV) $\lvert m_1\rvert$, $\lvert m_2\rvert$ (μ_B)	NM ΔE_{mag} (meV)	clustering ΔE (meV)
Mo/Cu			0 0.13 0.22	0	−123
Tc/Cu		0 0.00 0.12		0	−95
Ru/Cu	6 0.45 0.50	0 0.00 0.08		0	142
W/Cu			0 0.09 0.21	12	−68
Re/Cu		1 0.07 0.15		0	−92
Os/Cu				0	150

V. STRUCTURAL IMPERFECTIONS

The foregoing discussion assumed infinite, strictly linear nanowires, which are hardly realizable in real experiments. In reality diverse structural deficiencies such as fragmentation of the wires, clustering of the adatoms or diffusion of the adatoms into the substrate will be present and these can affect magnetism of nanowires dramatically. The ability to form perfect monoatomic wires depends on the balance between the surface and step energies of the substrate and of the deposited material which affect the growth mode and the quality of the nanopatterned structures. Because the surface energy of monovalent noble metals is smaller than that of $4d$ and $5d$ transition metals, if the surface is annealed or, alternatively, if the material is deposited at elevated temperatures, the deposited atoms will dissolve in surface layer. This means wires must be fabricated via a thermal nonequilibrium growth process at temperatures sufficiently low to prevent intermixing, but high enough such that the impinging atoms have already a sufficient mobility to diffuse towards and along steps. It has been pointed up that the best temperature range to grow nanowires is relatively narrow and can be quite different even for various species deposited on the same substrate.[6,7] In addition, referring back to Fig. 2, it is apparent that the nanowires are exposed to a considerable tensile strain. The difference in the interatomic bond length in bulk Ag and the calculated interatomic distances in an unsupported ferromagnetic Ru wire amounts to 24%, although the difference in the bond lengths between Ag and Ru solids is only 7%. Yet practical experience reveals that the conditions for an epitaxial relationship between the deposited wires and the underlying stepped surface are less stringent than for an overlayer growth because the atoms in wires are free to relax in two dimensions. Smooth monoatomic Co chains were grown on Pt(997), while in a monolayer Co/Pt(997) film a network of stacking faults develops.[7] It is noted that the lattice mismatch of Co and Pt equals to 10%.

Some aspects of the growth mode of nanowires have been studied in our recent work devoted to Fe wires on Cu(11n) substrates.[21] We have found that due to the strong heteroatomic Fe-Cu interactions, an Fe wire located below instead of at the step is energetically preferred. However, diffusion below the terraces is possible only through an atomic exchange process with a high activation energy — hence at not too high temperatures the Fe atoms will remain at the step edge. We have also examined the tendency of the adatoms to form clusters, comparing row-by-row versus island growth. In that case it turned out that the strong heteroatomic attraction was capable to stabilize row-by-row growth. Here we extend these studies to wires formed by the heavy transition metals.

A. Row-by-row versus island growth

An extended investigation of the growth mode would require very large models, larger than are now computationally affordable. Here we restrict ourselves to a very simple model: we compare the energies of continuous monoatomic wires with those of a stripe consisting of 2×2 clusters separated by an uncovered space of the same size, as illustrated in Fig. 1(b). Instead of a supercell with a periodicity of two nearest-neighbor distances along the wire as employed in the modeling of FM and AFM monoatomic wires, here we double our model to four bond lengths in the direction along steps and keep the terrace width fixed. We restricted ourselves to spin-compensated solutions. The negative energy differences ΔE between homogeneous monoatomic wires and (2×2) clusters listed in Tables IV and V are indicative of island formation, whereas in the systems with positive energy differences a row-by-row growth is expected.

From the energy differences it follows that on a copper substrate only Ru and Os among the examined atomic species tend to wet the steps. The other elements, at most Mo

TABLE V. The calculated magnetic moments m, the energy differences ΔE_{mag} with respect to the appropriate ground state solution for biatomic wires on Ag(117). The rightmost column represents the energy difference $\Delta E = E(\mathrm{cluster}) - E(\mathrm{wire})$ of the structural models drawn in Fig. 1. The energies are given per wire atom.

element	FM ΔE_{mag} (meV) m_1, m_2 (μ_B)	C-AFM ΔE_{mag} (meV) $\lvert m_1\rvert$, $\lvert m_2\rvert$ (μ_B)	R-AFM ΔE_{mag} (meV) $\lvert m_1\rvert$, $\lvert m_2\rvert$ (μ_B)	NM ΔE_{mag} (meV)	clustering ΔE (meV)
Nb/Ag	0	4	0	5	49
	0.24 0.55	0.09 0.30	0.25 0.53		
Mo/Ag	181	0	114	195	−51
	0.13 0.18	2.41 2.54	1.54 1.75		
Tc/Ag	991	0	423	1 656	−67
	1.30 2.12	2.25 2.36	2.27 2.43		
Ru/Ag	0	75	163	191	188
	1.95 2.02	1.81 1.88	0.86 1.44		
Rh/Ag	0		5	38	229
	0.94 0.96		0.71 0.69		
Pd/Ag				0	206
W/Ag	20	0	0	33	5
	0.34 0.60	1.41 1.52	0.79 0.89		
Re/Ag	110	0	65	100	25
	0.59 0.87	1.87 1.99	1.10 1.34		
Os/Ag	0	5	540	407	248
	0.86 1.63	1.16 1.41	1.45 1.37		
Ir/Ag	0		10	48	380
	1.02 1.04		0.52 0.48		
Pt/Ag				0	341

and Tc, prefer to nucleate spontaneously into islands. This is due to the fact that their mutual interaction is stronger than their bonding to the surface. Mo and Tc are also the sole elements for which an island growth on a silver template is predicted, although the energy difference between clustering and wire formation is reduced. W and Re tend to cluster on Cu(117), whereas on Ag(117) wire formation is marginally more favorable. For all other elements, row-by-row growth is found to be preferred on a Ag substrate.

The tendency to clustering does not seem to follow any transparent trend. There is no direct correlation to the bond lengths of the unsupported wires, or to the related step energies or the segregation energies. Quite generally, it can be inferred that for metals with a nearly half-filled band and hence a very large cohesive energy clustering prevails, whereas for early and late transition metals and weaker bonding forces wetting is favored. The fact that on Ag, i.e., on the substrate with the larger lattice spacing, more elements prefer a row-by-row growth is in line with the expectation of a more efficient stress relief in monoatomic wire in comparison to clusters. The most interesting cases from the perspective of growing magnetic $4d$ or $5d$ wires are Ru, Rh, and Os on a silver substrate as they meet the requirement of row-by-row growth combined with a substantial magnetic polarization. For Ru and Os on Cu, good row-by-row growth can be expected, but the ferromagnetic state has only marginal stability, the same also applies to Ir wires on Ag. For Re wires on Ag, a stable, strongly polarized magnetic ground state is expected, but the conditions for the growth of perfect monoatomic wires are more problematic.

B. From wires to films — biatomic stripes

The sensitivity of the magnetism of low-dimensional structures of $4d$ and $5d$ elements to changes in the local coordination is well established. The magnetism of monolayer magnetic films can be quenched by depositing a second layer as documented, e.g., for ruthenium films on silver substrates.[41] In this case the large magnetic moment in a Ru monolayer disappears completely on depositing a second Ru layer. The same happens for bilayers formed by other metals, the only exceptions seem to be Pt and Pd for which a weak magnetism sets in first in a bilayer film. On the other hand, the tendency towards magnetic ordering is promoted by the reduction of the dimension of the nanostructures, especially for the early transition elements with a less than half-filled band. As demonstrated by Bellini *et al.*,[19] the magnetic moment of Zr, Nb, Mo, and Tc on Ag(001) increases strongly on going from a monolayer to a monoatomic wire. The transition from wires to films, however, has not been investigated as of yet.

Prompted by these considerations we have examined the stability of the magnetic states found for monoatomic rows after another row is attached to them. We searched for a

ferromagnetic solution and two types of antiferromagnetic solutions, the first one with parallel magnetic moments within each chain but opposite between the chains (row-wise antiferromagnetism) and the second one with antiferromagnetic coupling to all nearest neighbors in the stripe (checkerboard antiferromagnetism). The calculations were performed for those elements that turned out to be magnetized in a monoatomic wire, adding Pt and Pd for the reasons mentioned above.

The calculated energy differences relative to the respective energy minimum, together with the magnetic moments are compiled in Table IV for biatomic stripes on Cu(117) and in Table V for the stripes on Ag(117). It is found that the interaction between the chains in the stripes on copper quenches the magnetic moments very efficiently. The magnetism surviving in Mo, Tc, W, and Ru stripes is likely too faint to be observable anyhow, and only for W stripes row-wise antiferromagnetism is stabilized by a small magnetic energy difference. For Ru stripes we find an enhancement of the magnetic moment compared to a monoatomic wire, but the ferromagnetic solution is only metastable. The main mechanism leading to the quenching of the magnetic moments is the reduction of the density of states at the Fermi level $N(E_F)$ induced by the broadening of the *d* bands resulting from the stronger hybridization between the atoms in the stripes, as they have higher coordination compared to the monoatomic rows. According to the Stoner theory of the band magnetism this reduces the tendency towards magnetism. This effect has been invoked many times in the literature when the correlations between the magnetism and the local structure have been in the center of interest.

On a Ag substrate, the antiferromagnetic wires and stripes of Nb (the FM and AFM solutions are energetically degenerate), Mo, Tc, W, and Re conform with this general picture as is apparent from Table V: both the magnetic moments and the magnetic energy differences are strongly reduced by the addition of a second row of adatoms. Generally, checkerboard antiferromagnetism is preferred over row-wise antiferromagnetism (in which part of the antiferromagnetic nearest-neighbor interactions are frustrated). However, under certain circumstances the broadening and smearing of the DOS due to hybridization may result in the elevated $N(E_F)$ and drive an enhancement of magnetic moments. This is nicely manifested by Ir stripes on silver (see Table V) which acquire moments that are two times larger than in a monoatomic wire, accompanied by an increase in the magnetic energy difference. The nonmagnetic DOS of the monoatomic Ir wire shows up two pronounced spikes, on every side of the Fermi level with a low between them falling on the Fermi level. After another row is added to the wire, the DOS maxima are broadened and $N(E_F)$ increases from 3.3 states/eV in the monoatomic wire to 3.5 states/eV in the biatomic stripe. A similar situation occurs for a Rh wire: $N(E_F)=3.3$ states/eV for a wire but $N(E_F)=4.6$ states/eV for a stripe. The third case where we find an increased $N(E_F)$ (from 1.6 to 1.9 states/eV) is Nb. However, because the *d* states of the early transition metals are more delocalized than the *d* states of the late transition metals, a slight enhancement of $N(E_F)$ in Nb is not accompanied by the larger magnetic moments. Further, a different degree of *d* states localization throughout the transition-metal series is responsible for larger differences between the inner and the outer magnetic moments for the elements at the begin of the series with respect to those from the end of the series. For Ru and Os we find only a small reduction of the magnetic moments of the biatomic stripes compared to the wires and comparable magnetic energy differences but note that for Os the addition of a second row dips the energetic balance in favor of ferromagnetic ordering. For Pd and Pt stripes the additional *d*-*d* hybridization leads to an increase of $N(E_F)$ (from 0.7 to 1.0 state/eV in Pd and from 0.9 to 1.8 states/eV in Pt). However, this is not sufficient to induce any magnetic ordering. For a biatomic Pt stripe on Ag(117) we obtained residual magnetic moments of $0.02\mu_B$, indicating that Pt stripes are at the edge of magnetism.

Clearly, the formation of thicker wires can influence the magnetism profoundly. For instance, a ferromagnetic free-standing Mo wire with the Ag bond length assumes a magnetic moment of $4.00\mu_B$. As the wire is placed onto Ag(117) substrate its moment is reduced to $2.36\mu_B$, and an addition of yet another row of Mo atoms results in further sizable reduction to about $0.15\mu_B$. In the complete Mo/Ag(001) overlayer a FM solution does not survive. When Mo moments are coupled antiferromagnetically, the following sequence is passed: $3.86\mu_B$ (free-standing wire), $3.00\mu_B$ [monoatomic wire on Ag(117)], about $2.47\mu_B$ [biatomic wire on Ag(117)], and $1.92\mu_B$ [2×2 AFM Mo/Ag(001) overlayer]. In the last case the 2×2 AFM state is by 59 meV/Mo atom below a row-wise AFM configuration (with the moment of $0.96\mu_B$) and by 70 meV lower than a nonmagnetic solution.

Direct evidence of the long-range magnetic order by probing the large-area magnetization of arrays of nanowires or stripes is complicated by the enormous sensitivity of the low-dimensional magnetism against all kinds of fluctuations. Techniques exploring the local magnetic state such as spin-resolved photoemission and inverse photoemission can be very helpful in searching for magnetism in nanowires on stepped surfaces. For this reason, we plotted the atom- and spin-resolved density of states of Ru on silver in Fig. 10. Visual inspection of the top panel showing the DOS of a nonmagnetic wire reveals a fairly simple structure with two peaks at -1.3 and 1 eV and one pronounced maximum at -0.2 eV. The origin of these structures has already been discussed above, the central peak results from the narrowing of the $dd\delta$ band as the interatomic distance in the wire is stretched to match the geometry of the substrate. In contrast, the DOS of a magnetized wire shows up a rippled structure with the deep minima at -1.8, -0.7, and 0.7 eV as the main characteristics. These structures result from the superposition of the spin-split one-dimensional DOS's, in which the structure of the $dd\delta$ band is better resolved than in the paramagnetic state. For comparison we show in Figs. 10(c) and 10(d) also the DOS's obtained for three-atom wide stripes covering each terrace completely and for a flat Ru/Ag(001) overlayer. Three characteristic minima are still present, although smeared and shifted to lower energies. All in all, the DOS

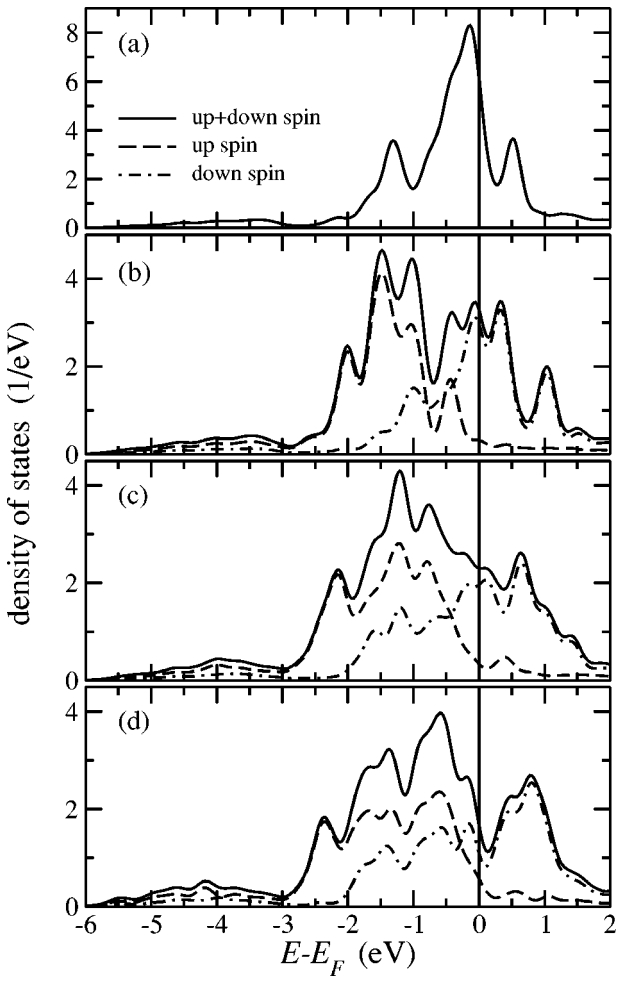

FIG. 10. Density of states of Ru on silver substrate in the form of (a) nonmagnetic wire, (b) ferromagnetic wire ($m=2.11\mu_B$), (c) ferromagnetic three-atom wide stripe ($\langle m\rangle=1.99\mu_B$), and (d) flat monolayer on silver ($m=1.94\mu_B$).

corresponding to the ferromagnetic Ru wire contains unique signatures to be resolved in photoemission spectra.

VI. CONCLUSIONS

The purpose of this work was to investigate the magnetic properties of linear ultrathin nanowires by applying density functional theory. The wires consist of the fifth and sixth row atoms, being nonmagnetic as bulk materials. In free-standing monoatomic $4d$ and $5d$ wires we find a parabolic dependence of the equilibrium bond length, corresponding to the progressive filling of first bonding and later antibonding d states. The electronic spectrum consists of a superposition of one-dimensional $dd\sigma$, $dd\pi$, and $dd\delta$ bands, with characteristic van Hove singularities. The narrowest of these bands, $dd\delta(d_{xy}+d_{x^2-y^2})$ is located close to the Fermi level. The position of the Fermi energy relative to the DOS maxima of this band leads to a transition from nonmagnetic to ferromagnetic and antiferromagnetic state and back to ferromagnetic and nonmagnetic state with d band filling, differing markedly from the trend in the bulk $3d$ metals. The fact that spin polarization affects mostly the transverse d_{xy} and $d_{x^2-y^2}$ bands is reflected in a magnetization density that is quite extended perpendicular to the wire, but localized in the direction along the wire.

Furthermore, we concentrated on the magnetism in wires located along the steps on Cu(117) and Ag(117) surfaces. In this geometry the interwire separation is 9.2 Å (on Cu) and 10.5 Å (on Ag). The binding of the wires to the steps is strongest for the half-filled transition-metal wires. The magnetism of supported wires is determined by three competing effects: (i) The tensile strain imposed by the epitaxial relation with the substrate favors magnetism, but can also lead to a reduction of the energy difference between ferromagnetic and antiferromagnetic wires. (ii) The increased coordination gives rise to a band broadening. (iii) Hybridization of the d bands of wire and substrate shifts the d states of the wire towards the Fermi level. This shift is more pronounced on Cu than on Ag. The result is quite remarkable — on Cu(117) not only the wires formed by the elements of the Fe group, but also those formed by the Cr- and Mn-group elements order ferromagnetically. This is a consequence of the hybridization-induced d band shift. On Ag(117) on the other hand, antiferromagnetic order is found even for the heaviest element of the Fe group Os.

In $3d$ metals and their alloys an empirical correlation between the magnetic exchange splitting between spin-up and spin-down d bands and the resulting magnetic moment was observed, viz. the exchange splitting scales linearly with the moments with about 1 eV per Bohr magneton.[39,40] The values of Stoner parameter I in magnetic wires on stepped surfaces reveal that this relation is preserved to a rather good approximation also in $4d$ and $5d$ elements taking $I=0.7\pm0.1$ eV/μ_B.

Another row of atoms added to the wires quenches magnetism in wires on Cu substrate and decreases it in the wires on Ag substrate. The exceptions are Rh and Ir biatomic stripes in which an enhancement of magnetic moments takes place. To assess the stability of the wire geometry and the ability to grow perfect monoatomic wires, we studied another structure with small clusters at the step edges. It is found that the wire geometry is largely preferred, particularly on Ag substrate, whereas on Cu substrate a tendency to clustering prevails.

Linking all the results together, Ru, Rh, and Os wires on Ag(117) are suggested as the most promising systems in which magnetism could be verified experimentally. We hope, the outcomes presented in this paper will provide some guidance to experimental efforts to grow nanowires and to achieve novel magnetic nanostructures.

ACKNOWLEDGMENTS

This work has been supported by the Austrian Science Funds under Project No. 16184-N02. The calculations were performed on Schrödinger I computer system at the Computer Center of Vienna University.

*Email address: Daniel.Spisak@univie.ac.at

[1] L.P. Regnault, I. Zaliznyak, J.P. Renard, and C. Vettier, Phys. Rev. B **50**, 9174 (1994), and references therein.
[2] H.J. Elmers, J. Hauschild, H. Höche, U. Gradmann, H. Bethge, D. Heuer, and U. Köhler, Phys. Rev. Lett. **73**, 898 (1994).
[3] T. Jung, R. Schlittler, J.K. Gimzewski, and F.J. Himpsel, Appl. Phys. A: Mater. Sci. Process. **61**, 467 (1995).
[4] J. Shen, R. Skomski, M. Klaua, H. Jenniches, S. Sundar Manoharan, and J. Kirschner, Phys. Rev. B **56**, 2340 (1997).
[5] V. Repain, J.M. Berroir, S. Rousset, and J. Lecoeur, Surf. Sci. **447**, L152 (2000).
[6] P. Gambardella, M. Blanc, H. Brune, K. Kuhnke, and K. Kern, Phys. Rev. B **61**, 2254 (2000).
[7] P. Gambardella, M. Blanc, L. Bürgi, K. Kuhnke, and K. Kern, Surf. Sci. **449**, 93 (2000).
[8] P. Gambardella, A. Dallmeyer, K. Maiti, M.C. Malagoll, W. Eberhardt, K. Kern, and C. Carbone, Nature (London) **416**, 301 (2002).
[9] G. Rubio, N. Agrait, and S. Vieira, Phys. Rev. Lett. **76**, 2302 (1996).
[10] H. Ohnishi, Y. Kondo, and K. Takayanagi, Nature (London) **395**, 780 (1998).
[11] A.I. Yanson, G. Rubio-Bollinger, H.E. van den Brom, N. Agrait, and J.M. van Ruitenbeek, Nature (London) **395**, 783 (1998).
[12] D.I. Paul, Phys. Rev. **118**, 92 (1960); *ibid.* **120**, 463 (1960).
[13] E. Lieb and D. Mattis, Phys. Rev. **125**, 164 (1962).
[14] M. Weinert and A. J. Freeman, J. Magn. Magn. Mater. **38**, 23 (1983).
[15] N. Zabala, M.J. Puska, and R.M. Nieminen, Phys. Rev. Lett. **80**, 3336 (1998).
[16] A. Ayuela, H. Raebiger, M.J. Puska, and R.M. Nieminen, Phys. Rev. B **66**, 035417 (2002).
[17] S. Okada and A. Oshiyama, Phys. Rev. B **62**, R13 286 (2000).
[18] A. Bergara, J.B. Neaton, and N.W. Ashcroft, Int. J. Quantum Chem. **91**, 239 (2003).
[19] V. Bellini, N. Papanikolaou, R. Zeller, and P.H. Dederichs, Phys. Rev. B **64**, 094403 (2001).
[20] M. Eisenbach, B.L. Györffy, G.M. Stocks, and B.L. Újfalussy, Phys. Rev. B **65**, 144424 (2002).
[21] D. Spišák and J. Hafner, Phys. Rev. B **65**, 235405 (2002).
[22] S. Blügel, Phys. Rev. Lett. **68**, 851 (1992).
[23] G. Kresse and J. Furthmüller, Phys. Rev. B **54**, 11 169 (1996); Comput. Mater. Sci. **6**, 15 (1996).
[24] P. Blöchl, Phys. Rev. B **50**, 17 953 (1994).
[25] G. Kresse and D. Joubert, Phys. Rev. B **59**, 1758 (1999).
[26] J. Perdew and A. Zunger, Phys. Rev. B **23**, 5048 (1981).
[27] S.H. Vosko, L. Wilk, and M. Nusair, Can. J. Phys. **58**, 1200 (1980).
[28] J.P. Perdew, J.A. Chevary, S.H. Vosko, K.A. Jackson, M.R. Pedersen, D.J. Singh, and C. Fiolhais, Phys. Rev. B **46**, 6671 (1992).
[29] Detailed informations on the VASP code and the database on PAW potentials may be found at http://cms.mpi.univie.ac.at/vasp/
[30] L. De Maria and M. Springborg, Chem. Phys. Lett. **323**, 293 (2000).
[31] K. Schmidt and M. Springborg, Solid State Commun. **104**, 413 (1997).
[32] H.J. Monkhorst and J.D. Pack, Phys. Rev. B **13**, 5188 (1976).
[33] D.G. Pettifor, *Bonding and Structure of Molecules and Solids* (Clarendon Press, Oxford 1995).
[34] V. Heine and J.H. Samson, J. Phys. F: Met. Phys. **13**, 2155 (1983).
[35] R. Hoffmann, Rev. Mod. Phys. **60**, 601 (1988).
[36] G. Brocks, P.J. Kelly, and R. Car, Phys. Rev. Lett. **70**, 2786 (1993).
[37] M.A. van Hove and G.A. Somorjai, Surf. Sci. **92**, 489 (1980).
[38] P. Oelhafen, in *Glassy Metals II*, edited by H. Beck and H.J. Güntherodt (Springer, Berlin 1983), 283.
[39] F.J. Himpsel, Phys. Rev. Lett. **67**, 2363 (1991).
[40] I. Turek, Ch. Becker, and J. Hafner, J. Phys.: Condens. Matter **4**, 7257 (1992).
[41] S. Blügel, Phys. Rev. B **51**, 2025 (1995).